

Seasonal Variations of Surface $f\text{CO}_2$ and Sea-Air CO_2 Fluxes in the Ulleung Basin of the East/Japan Sea

Sang-Hwa Choi¹, Dongseon Kim^{2,*}, JeongHee Shim³, Kyung-Hee Kim², Hong Sik Min²,
and Kyung-Ryul Kim⁴

¹ Ocean Data and Information Unit, Korea Ocean Research and Development Institute, Seoul, Korea

² Climate Change and Coastal Disaster Research Department, Korea Ocean Research and Development Institute, Seoul, Korea

³ Environment Research Division, National Fisheries Research and Development Institute, Busan, Korea

⁴ School of Earth and Environmental Sciences, Seoul National University, Seoul, Korea

Received 8 August 2011, accepted 19 January 2012

ABSTRACT

Temperature, salinity, chlorophyll *a*, and surface CO_2 fugacity ($f\text{CO}_2$) were extensively investigated in the Ulleung Basin of the East/Japan Sea during four seasonal cruises. In spring, surface $f\text{CO}_2$ showed large variations ranging from 260 to 356 μatm , which were considerably lower than the atmospheric CO_2 levels. Surface $f\text{CO}_2$ was highest (316 to 409 μatm) in summer. The central part of the study area was undersaturated with respect to atmospheric CO_2 , while the coastal and easternmost regions were oversaturated. In autumn, the entire study area was fairly undersaturated with respect to atmospheric CO_2 . In winter, surface $f\text{CO}_2$ ranged from 303 to 371 μatm , similar to that in autumn, despite the much lower sea surface temperature. The seasonal variation in surface $f\text{CO}_2$ could not be explained solely by seasonal changes in sea surface temperature and salinity. The vertical mixing, lateral transport, and sea-air CO_2 exchange considerably influenced the seasonal variation in surface $f\text{CO}_2$. The Ulleung Basin of the East/Japan Sea was a sink of atmospheric CO_2 in spring, autumn, and winter, but a weak source of CO_2 to the atmosphere in summer. The annual integrated sea-air CO_2 flux in the Ulleung Basin of the East/Japan Sea was $-2.47 \pm 1.26 \text{ mol m}^{-2} \text{ yr}^{-1}$, quite similar to a previous estimate ($-2.2 \text{ mol m}^{-2} \text{ yr}^{-1}$) in the south East/Japan Sea. This indicates that the Ulleung Basin of the East/Japan Sea acts as a strong sink of atmospheric CO_2 .

Key words: Seasonal variations, Surface $f\text{CO}_2$, Sea-air CO_2 flux, Marginal sea, CO_2 sink

Citation: Choi, S. H., D. Kim, J. H. Shim, K. H. Kim, H. S. Min, and K. R. Kim, 2012: Seasonal variations of surface $f\text{CO}_2$ and sea-air CO_2 fluxes in the Ulleung Basin of the East/Japan Sea. *Terr. Atmos. Ocean. Sci.*, 23, 343-353, doi: 10.3319/TAO.2012.01.19.01(Oc)

1. INTRODUCTION

Marginal seas play important roles in the global carbon cycle, with those having high biological activities serving as annual net sinks (Borges et al. 2005; Omar et al. 2007; Chen and Borges 2009). However, while marginal seas at temperate and high latitudes act as net sinks, those at tropical and subtropical latitudes may act as net sources (Borges et al. 2005; Chen and Borges 2009). Previous studies on the sea-air CO_2 fluxes of marginal seas have reported large variability ranging from $0.1 \sim 0.45 \text{ Pg C yr}^{-1}$, which is attributable to the complex and heterogeneous ecosystems and hydrodynamics of these seas (Liu et al. 2000; Thomas et al. 2004; Borges et al. 2005; Chen and Borges 2009). For

the same reason, estimates of sea-air CO_2 flux for marginal seas still contain much uncertainty. Therefore, spatially and temporally high-resolution CO_2 measurements in marginal seas are essential for improving estimates of global sea-air CO_2 fluxes.

The East/Japan Sea (hereafter, East Sea) is a semi-enclosed marginal sea surrounded by Korea, Japan, and Russia. It consists of three major basins: the Japan, Yamato, and Ulleung basins. The average depth of the East Sea is 1740 m, and it connects to the western North Pacific through four shallow straits with depths less than 140 m. Because of the shallow depths of these straits, subsurface waters below the thermocline (located at about 100 ~ 200 m) cannot be directly exchanged between the East Sea and North Pacific. Due to high biological productivity and accumulation of anthropogenic CO_2 (Yamada et al. 2005; Park et al. 2006; Yoo

* Corresponding author
E-mail: dkim@kordi.re.kr

and Park 2009), the East Sea could be an important marginal sea in which to study oceanic carbon cycles. However, relatively few studies have investigated sea-air CO₂ fluxes in the southwestern part of the East Sea, the Ulleung Basin (Oh 1998; Kang 1999; Choi et al. 2011). Oh (1998) and Kang (1999) estimated daily and monthly averaged sea-air CO₂ flux in the East Sea using a multifactor mathematical model tuned by observational data in summer and winter. Choi et al. (2011) reported the surface *f*CO₂ distribution and sea-air CO₂ flux in the Ulleung Basin of the East Sea in the summer of 2005. Until now, however, seasonal observations of sea-air CO₂ fluxes have not been performed in the East Sea.

We investigated the spatial distribution and seasonal variations of surface *f*CO₂ in the Ulleung Basin of the East Sea based on data obtained in April 2006, August 2007, and February and October 2008. Here we evaluate the major physical and biological factors controlling the distribution of surface *f*CO₂ in the study area, and estimate the sea-air CO₂ fluxes for four seasonal surveys.

2. MATERIALS AND METHODS

2.1 Analytical Methods

The data were obtained during four seasonal cruises on board the R/V *Eardo* in spring (15 ~ 16 April 2006), summer (5 ~ 9 August 2007), autumn (9 ~ 14 October 2008), and winter (20 ~ 23 February 2008). The study area was the Ulleung Basin of the East Sea (35 ~ 37°N, 129 ~ 132°E, Fig. 1). Continuous measurements were made of *f*CO₂, temperature, and salinity in the surface seawater, which was pumped aboard from a 5-m depth during the surveys. Surface *f*CO₂ and atmospheric CO₂ were determined every minute and every hour, respectively, using an underway CO₂ measurement system consisting of a flowing *p*CO₂ system and a showerhead equilibrator. The *f*CO₂ measurements were described in detail by Shim et al. (2007). The system was calibrated every 12 hours with working standard gases (~250, 380, and 450 ppm CO₂ in the air, Korea Industrial Gases, Ltd., Shihung City, Korea), which were subsequently calibrated with the National Oceanic and Atmospheric Administration (NOAA) and World Meteorological Organization (WMO). Consistency between pre- and post-cruise analyses for the working standard gases was 1 μatm. Repeated analyses also indicated that the *f*CO₂ measurement had a precision of ±1 μatm. Vertical profiles of temperature, salinity, and density were measured with a SeaBird conductivity-temperature-depth profiler (CTD; SBE 9/11 plus, SeaBird Inc., Bellevue, WA, USA). Seawater samples for chlorophyll *a* analyses were collected using a Rosette sampler with 10-L Niskin bottles. The seawater for the chlorophyll *a* analysis was filtered through GF/F filter paper (47 mm, Whatman), and the filters were then immediately frozen using liquid nitrogen. The chlorophyll *a* concentra-

tion in the extracted filtrate mixed with 90% acetone for 24 h was determined using a Turner-designed fluorometer (10-006R, Turner BioSystems, Sunnyvale, CA, USA).

2.2 Calculation of the Sea-Air CO₂ Flux

The sea-air CO₂ fluxes across the sea-air interface can be calculated based on the equation $F = k \times s \times \Delta f\text{CO}_2$, where *k* is the gas transfer velocity (cm h⁻¹), *s* is the solubility of CO₂ gas in seawater (mol kg⁻¹ atm⁻¹; Weiss 1974), and Δ*f*CO₂ is the sea-air difference of CO₂ fugacity. A positive flux indicates that the sea is acting as a CO₂ source; a negative flux means that the sea is acting as a CO₂ sink. We adapted the formula for *k* and the wind speed relationships from Wanninkhof (1992) to allow comparison of our results with those of most other studies. Wind speed is the key force driving gas exchange at the sea-air interface. Here, we used the spatially averaged QuikSCAT wind speed data for the cruise dates, obtained from the Physical Oceanography Distributed Active Archive Center of the Jet Propulsion Laboratory, US National Aeronautics and Space Administration (PO.DAAC, JPL, NASA: <http://podaac.jpl.nasa.gov>).

3. RESULTS AND DISCUSSION

3.1 Surface Currents in the Ulleung Basin of the East Sea

The Ulleung Basin is located in the southwestern part of the East Sea. Although the Korea/Tsushima Strait is the only entrance to the Ulleung Basin, several surface currents

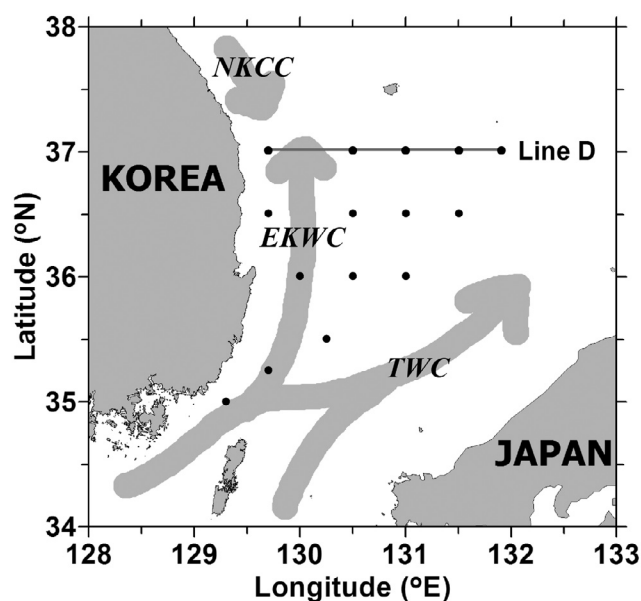


Fig. 1. Study area and locations of sampling stations in the East/Japan Sea. TWC indicates the Tsushima Warm Current, EKWC East Korea Warm Current, and NKCC North Korea Cold Current.

occur in the basin. The Tsushima Warm Current branches from the Kuroshio Current into the Ulleung Basin and then splits into two or three branches (Chang et al. 2002). Especially in summer, the Tsushima Warm Current carries both warm, low salinity water originating from the shelf of the East China Sea and high salinity water of Kuroshio origin (Chang et al. 2004). The northward branch along the east coast of Korea has been called the East Korean Warm Current (Uda 1934).

Figure 2 shows the surface temperature and salinity overlaid with currents for the four survey periods from the hybrid coordinate ocean model (HYCOM, <http://www.hycom.org/dataserver/glb-analysis>). In spring (April 2006), the Tsushima Warm Current, which had salinity higher than 34.4, passed along the Japanese coast, and there was a distinct anticyclonic eddy with 10°C core temperature and 34.2 salinity in the center of the Ulleung Basin (Figs. 2a and e). In summer (August 2007), the Tsushima Warm Current transported warm ($> 25^\circ\text{C}$) and less saline (< 33.2) water into the Ulleung Basin through both channels in the Korea/Tsushima Strait (Figs. 2b and f). In autumn (October 2008), the Tsushima Warm Current became weaker than in summer, and an anticyclonic eddy also became weaker (Figs. 2c and g). In winter (February 2008), the surface current through the Korea/Tsushima Strait was the weakest, but an anticyclonic eddy was well developed compared to other seasons (Figs. 2d and h). The surface temperature in the Ulleung Basin was warmer in winter than in spring.

3.2 Spatial and Seasonal Variations of Surface $f\text{CO}_2$

Surface $f\text{CO}_2$ is determined as a function of physical factors (temperature and salinity), chemical factors (dissolved inorganic carbon, DIC and total alkalinity, TA), and others (vertical mixing, lateral mixing, biological uptake, sea-air CO_2 exchange, etc.). $f\text{CO}_2$ is expressed approximately as

$$f\text{CO}_2 \approx Nf\text{CO}_{2\text{ave}}(T_{\text{ave}}, S_{\text{ave}}) + \Delta f\text{CO}_2(T_{\text{obs}} - T_{\text{ave}}) + \Delta f\text{CO}_2(S_{\text{obs}} - S_{\text{ave}}) + \Delta Nf\text{CO}_2(T_{\text{ave}}, S_{\text{ave}}) \quad (1)$$

where $Nf\text{CO}_{2\text{ave}}(T_{\text{ave}}, S_{\text{ave}})$ represents the mean temperature- and salinity-normalized $f\text{CO}_2$, $\Delta f\text{CO}_2(T_{\text{obs}} - T_{\text{ave}})$ the thermodynamic effect of SST change on $f\text{CO}_2$, $\Delta f\text{CO}_2(S_{\text{obs}} - S_{\text{ave}})$ the thermodynamic effect of salinity change on $f\text{CO}_2$, and $\Delta Nf\text{CO}_2(T_{\text{ave}}, S_{\text{ave}})$ the change in the normalized $f\text{CO}_2$ due to the changes in non-thermodynamic effect of changes in DIC, TA, vertical mixing, lateral mixing, biological uptake, and sea-air CO_2 exchange, etc. The value of $\Delta Nf\text{CO}_2(T_{\text{ave}}, S_{\text{ave}})$ is thus obtained from

$$\Delta Nf\text{CO}_2(T_{\text{ave}}, S_{\text{ave}}) \approx f\text{CO}_2 - Nf\text{CO}_{2\text{ave}}(T_{\text{ave}}, S_{\text{ave}}) - \Delta f\text{CO}_2(T_{\text{obs}} - T_{\text{ave}}) - \Delta f\text{CO}_2(S_{\text{obs}} - S_{\text{ave}}) \quad (2)$$

For the normalization of SST and SSS, we used the $f\text{CO}_2$ -SST and $f\text{CO}_2$ -SSS relationships of Takahashi et al. (1993):

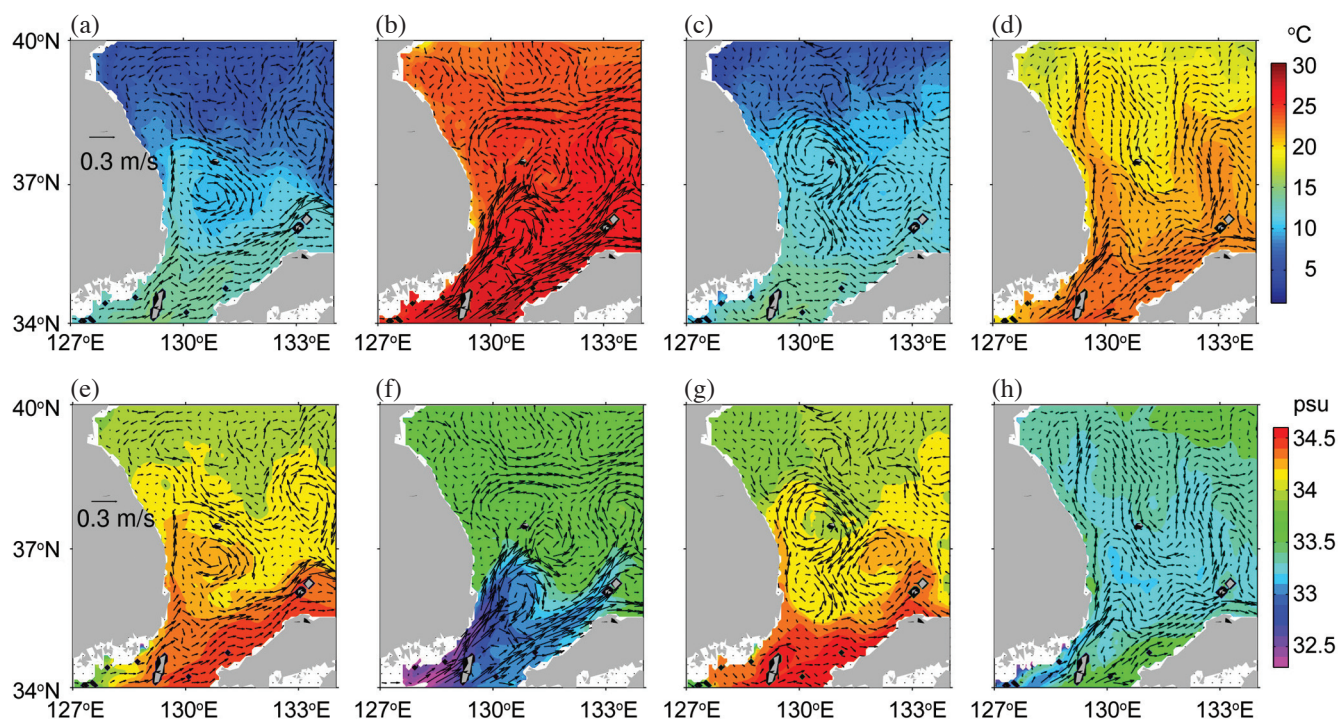


Fig. 2. Surface distribution of temperature overlaid with surface currents in April 2006 (a), August 2007 (b), October 2008 (c), and February 2008 (d) and salinity overlaid with surface currents in April 2006 (e), August 2007 (f), October 2008 (g), and February 2008 (h) from HYCOM.

$(dfCO_2/dT)/fCO_2 = 0.0423\text{ }^\circ\text{C}^{-1}$, $(dfCO_2/dS)(S/fCO_2) = 0.94$. Thermodynamic effect ratio for spatial distribution (TER_{spatial}) of each season is a ratio of sheer fCO_2 change by a thermodynamic effect of SST and SSS variations to total fCO_2 change by thermodynamic and non-thermodynamic effect ($(|\Delta fCO_2(T_{\text{obs}} - T_{\text{ave}})| + |\Delta fCO_2(S_{\text{obs}} - S_{\text{ave}})|) / (|\Delta fCO_2(T_{\text{obs}} - T_{\text{ave}})| + |\Delta fCO_2(S_{\text{obs}} - S_{\text{ave}})| + |\Delta NfCO_2(T_{\text{ave}}, S_{\text{ave}})|)$) using a seasonal mean of SST and SSS. The thermodynamic effect ratio for seasonal change (TER_{seasonal}) is the same as above using annual mean of SST and SSS instead of seasonal mean. The surface distributions of temperature, salinity, fCO_2 , and chlorophyll a for the four cruises are shown in

Fig. 3. In spring (April 2006), surface measurements were conducted in a narrow area covering from 129.5 to 131.5°E along 37°N. Due to the narrow coverage, the sea surface temperature (SST) and salinity (SSS) were confined to within a narrow range from 9.4 to 11.7°C and from 34.2 to 34.5, respectively (Figs. 3a and b). However, surface fCO_2 showed large variations, ranging from 260 to 356 μatm , which were considerably lower than atmospheric CO_2 (376.6 μatm). The $\Delta fCO_2(T_{\text{obs}} - T_{\text{ave}})$, $\Delta fCO_2(S_{\text{obs}} - S_{\text{ave}})$, $\Delta NfCO_2(T_{\text{ave}}, S_{\text{ave}})$, TER_{spatial} , and TER_{seasonal} for the four cruises are shown in Fig. 4. $\Delta fCO_2(T_{\text{obs}} - T_{\text{ave}})$ and $\Delta fCO_2(S_{\text{obs}} - S_{\text{ave}})$ were in small ranges, from -17 to 13 μatm and from -2 to 1 μatm ,

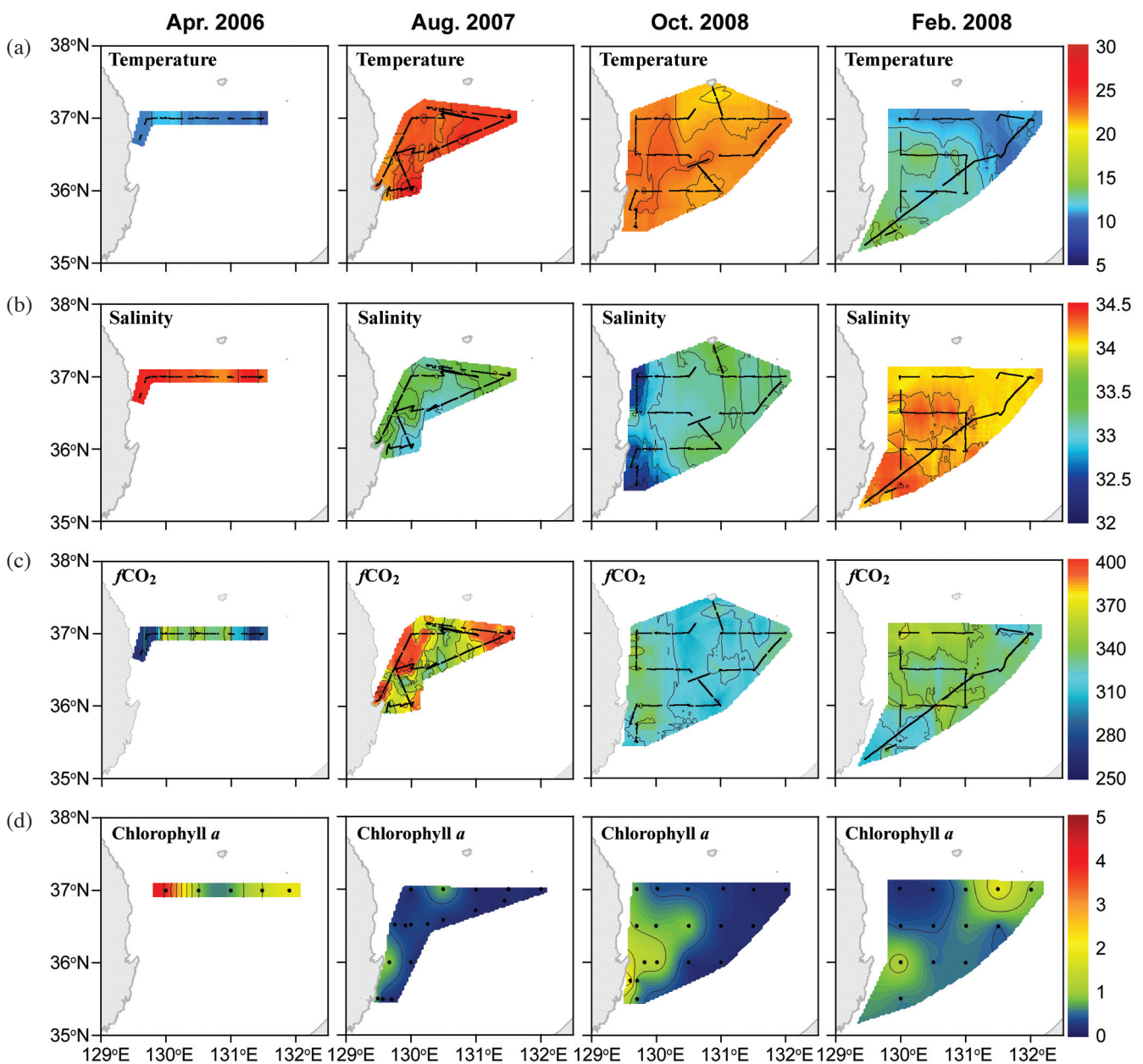


Fig. 3. Surface distribution of temperature (a), salinity (b), fCO_2 (c), and chlorophyll a (d) in April 2006, August 2007, October 2008, and February 2008.

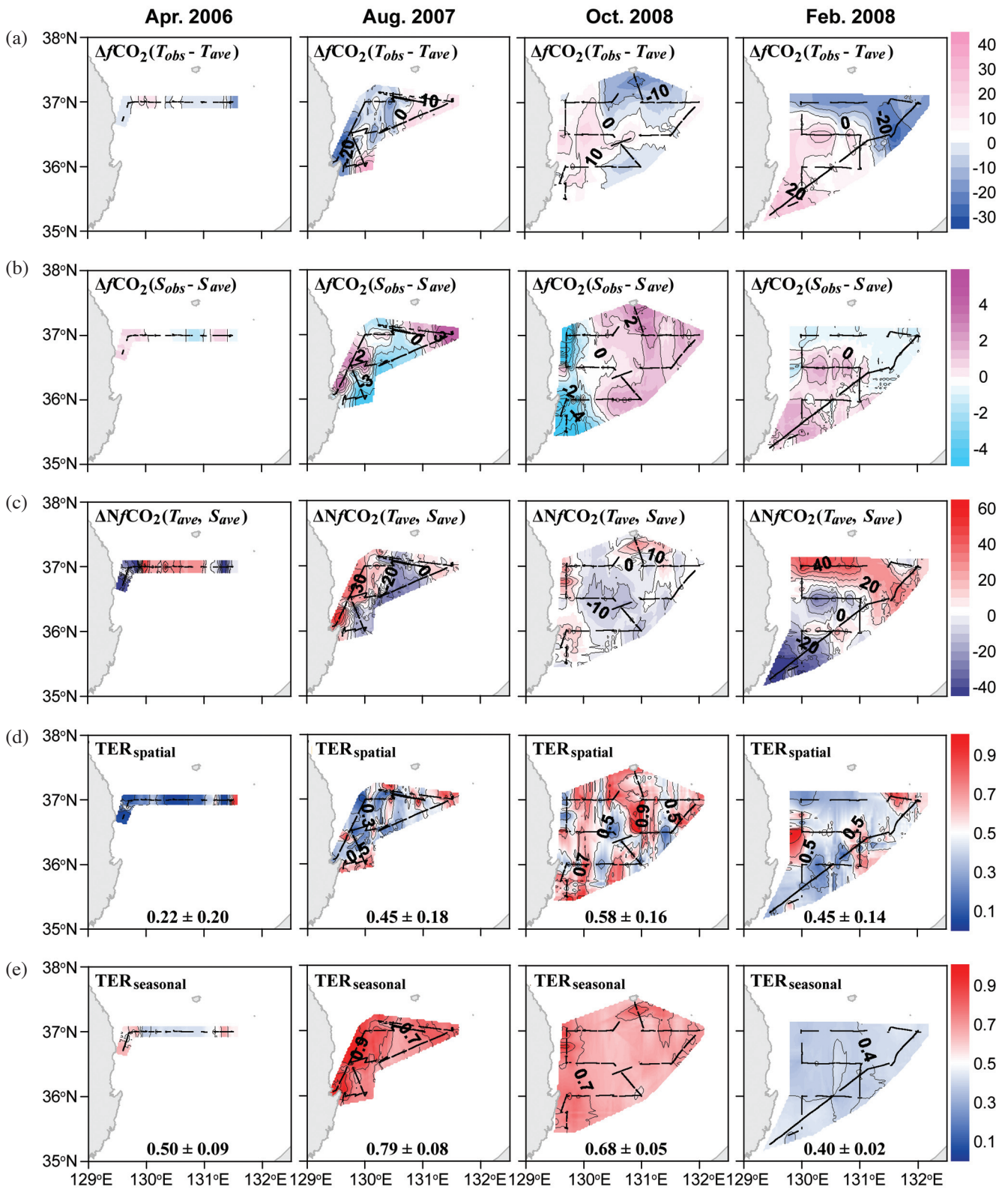


Fig. 4. Surface distribution of $\Delta f\text{CO}_2 (T_{obs} - T_{ave})$ (a), $\Delta f\text{CO}_2 (S_{obs} - S_{ave})$ (b), $\Delta Nf\text{CO}_2 (T_{ave}, S_{ave})$ (c), $\text{TER}_{\text{spatial}}$ (d), and $\text{TER}_{\text{seasonal}}$ (e) in April 2006, August 2007, October 2008, and February 2008. $\text{TER}_{\text{spatial}}$ (thermodynamic effect ratio for spatial distribution) of each season is a ratio of sheer $f\text{CO}_2$ change by thermodynamic effect of SST and SSS variation to total $f\text{CO}_2$ change by thermodynamic and non-thermodynamic effect ($(|\Delta f\text{CO}_2 (T_{obs} - T_{ave})| + |\Delta f\text{CO}_2 (S_{obs} - S_{ave})|) / (|\Delta f\text{CO}_2 (T_{obs} - T_{ave})| + |\Delta f\text{CO}_2 (S_{obs} - S_{ave})| + |\Delta Nf\text{CO}_2 (T_{ave}, S_{ave})|)$) using a seasonal mean of SST and SSS. $\text{TER}_{\text{seasonal}}$ (thermodynamic effect ratio for seasonal change) is the same as above using annual mean of SST and SSS. The figures in (d) and (e) represent the mean \pm standard deviation (S.D.).

respectively, whereas $\Delta NfCO_2(T_{ave}, S_{ave})$ was a large range, from -57 to $59 \mu\text{atm}$ (Figs. 4a, b and c). Thus, TER_{spatial} was as low as 0.22 ± 0.20 , implying that SST and SSS were not the major factors in controlling the spatial distribution of surface fCO_2 in spring (Fig. 4d). Among non-thermodynamic factors controlling surface fCO_2 , vertical and lateral mixing, and sea-air CO_2 exchange will be discussed in section 3.3. Lower surface fCO_2 (less than $300 \mu\text{atm}$) was observed in the area where chlorophyll a concentrations in the surface waters were relatively high (Figs. 3c and d). Figure 5 shows the relationship between $\Delta NfCO_2(T_{ave}, S_{ave})$ and surface chlorophyll a for the four surveys. The changes of normalized fCO_2 by non-thermodynamic factors showed a strong negative correlation with chlorophyll a only in spring ($r^2 = 0.75$). It suggested that spatial distribution of surface fCO_2 is largely influenced by biological activities in spring.

In summer (August 2007), SST showed a wide range from 21.4 to 26.2°C , and SSS varied from 32.8 to 33.8 (Figs. 3a and b). Surface fCO_2 had a wide range from 316 to $409 \mu\text{atm}$, the highest among the four seasons (Fig. 3c). Lower surface fCO_2 was observed in the central part of the study area where SSS was also relatively low (< 33.0). Despite that a variation of $\Delta fCO_2(T_{obs} - T_{ave})$ became larger than that in spring, ranging from -36 to $38 \mu\text{atm}$, spatial distribution of surface fCO_2 was much more similar to $\Delta fCO_2(S_{obs} - S_{ave})$ (Figs. 4a and b). Spatial distribution of $\Delta NfCO_2(T_{ave}, S_{ave})$ corresponded with that of $\Delta fCO_2(S_{obs} - S_{ave})$ (Figs. 4b and c). Moreover, $\Delta NfCO_2(T_{ave}, S_{ave})$ showed a larger range from -48 to $62 \mu\text{atm}$ than both $\Delta fCO_2(T_{obs} - T_{ave})$, from -36 to $38 \mu\text{atm}$ and $\Delta fCO_2(S_{obs} - S_{ave})$, from -5 to $5 \mu\text{atm}$. Thus, TER_{spatial} was 0.45 ± 0.18 , representing SST and SSS were not the primary factors to determine the spatial distribution of surface fCO_2 in summer (Fig. 4d). The Tsushima Warm Current became less saline in summer because it included low salinity shelf water from the East China Sea. Furthermore, the Changjiang Diluted Water could reach the East Sea through the Korea Strait in summer (Chen et al. 2003). Wang and Chen (1996) reported that the normalized alkalinity ($NTA = TA \times 35/S$) and salinity had a linear relationship with NTA shooting up (up to $2480 \mu\text{mol kg}^{-1}$; normal range of surface NTA in the East China Sea and East Sea was $2320 \sim 2360 \mu\text{mol kg}^{-1}$) at lower salinity by riverine alkalinity input in the shelf area of the East China Sea. High NTA and low DIC of surface water might be the major non-thermodynamic factors to diminish the surface fCO_2 in summer. The central part of the study area was undersaturated with respect to atmospheric CO_2 ($371.0 \mu\text{atm}$), whereas oversaturation was observed in coastal regions and in the far east of the study area. Oversaturation was found only in summer. Choi et al. (2011) measured surface fCO_2 in the Ulleung Basin of the East Sea on July 2005 and reported that the western and eastern parts of the Ulleung Basin were oversaturated with respect to atmospheric CO_2 , while the central part was undersaturated. They suggested that the

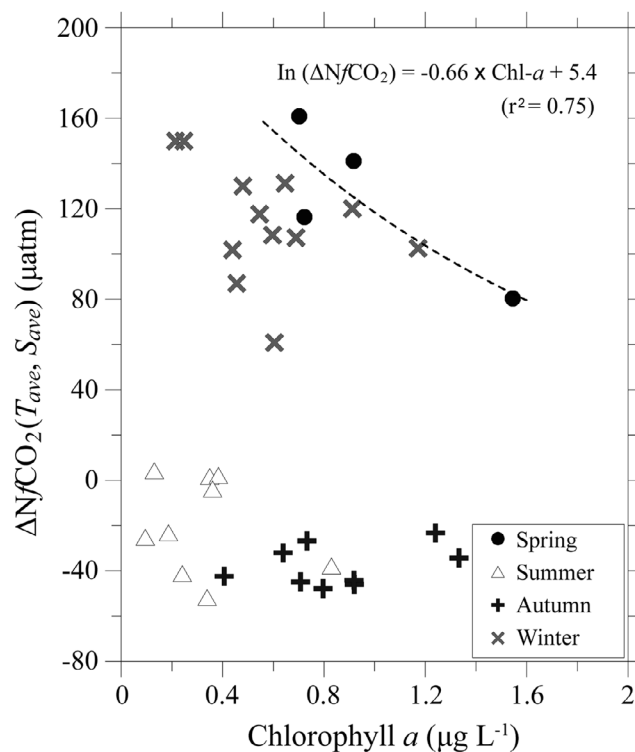


Fig. 5. Relationship between $\Delta NfCO_2(T_{ave}, S_{ave})$ and surface chlorophyll a for the four seasonal surveys.

undersaturation resulted from low SSS and high biological activity. In this study, relatively high surface chlorophyll a concentrations were also observed in the central region (Fig. 3d). A rough anti-correlation showed between $\Delta NfCO_2(T_{ave}, S_{ave})$ and surface chlorophyll a (Fig. 5), indicating that biological activity slightly influenced the spatial variability of surface fCO_2 in summer.

In autumn (October 2008), SST ranged from 20.4 to 23.8°C , somewhat lower than in summer, and SSS varied from 32.3 to 33.6 , rather similar to that in summer (Figs. 3a and b). Less saline waters were observed in the coastal regions; these waters were probably associated with the East Korea Warm Current that branches from the Tsushima Warm Current (Chang et al. 2004). Surface fCO_2 ranged from 298 to $355 \mu\text{atm}$, a somewhat lower variation than in summer (Fig. 3c). In autumn, the study area was fairly undersaturated with respect to atmospheric CO_2 ($376.6 \mu\text{atm}$). Lower surface fCO_2 was observed in the central part of the study area, which was characterized by moderate SST, SSS, and surface chlorophyll a . $\Delta NfCO_2(T_{ave}, S_{ave})$ showed a smallest range from -20 to $40 \mu\text{atm}$ among 4 seasonal observations (Fig. 4c). TER_{spatial} was 0.58 ± 0.16 , which was the highest value (Fig. 4d). It meant that SST and SSS were the major factors to control the surface fCO_2 in autumn. Distributions of $\Delta fCO_2(T_{obs} - T_{ave})$ and $\Delta fCO_2(S_{obs} - S_{ave})$ were almost opposite in phase, thus the variations of surface fCO_2 by SST and SSS changes were canceled out (Figs. 4a and b). Due

to both a compensation of surface $f\text{CO}_2$ variation by SST and SSS changes, and small amount of non-thermodynamic effect on surface $f\text{CO}_2$, surface $f\text{CO}_2$ in the central part of the study area was low. Surface $f\text{CO}_2$ was relatively high in the coastal areas, where SSS was relatively low and surface chlorophyll a concentrations were high (Figs. 3b, c and d). In summer, low SSS and high chlorophyll a led to a decrease in surface $f\text{CO}_2$, but these two factors were less important for controlling surface $f\text{CO}_2$ in autumn. $\Delta Nf\text{CO}_2 (T_{ave}, S_{ave})$ was high in the coastal area where SSS was low (Figs. 3b and 4d). In the coastal areas where the water's depth was shallow, vertical mixing actively occurred in autumn when the surface stratification was weakened by the decrease in SST. In this study, the mixed layer depth increased from 10 m in summer to 25 m in autumn. It was deeper in the coastal areas than offshore (Fig. 6). Thus, the high surface $f\text{CO}_2$ in coastal areas was ascribed to vertical mixing, which brought CO_2 -rich subsurface waters to the surface. Shim et al. (2007) suggested that the high surface $f\text{CO}_2$ in the northern East China Sea in autumn was the result of vertical mixing with deep waters rich in CO_2 .

In winter (February 2008), the SST ranged from 10.1 to 14.4°C, about 10°C lower than in autumn, and SSS varied from 34.0 to 34.4, somewhat higher than in autumn (Figs. 3a and b). Surface $f\text{CO}_2$ in winter ranged from 303 to 371 μatm , quite similar to that in autumn, despite the much lower SST (Fig. 3c). $\Delta f\text{CO}_2 (S_{obs} - S_{ave})$ varied in a small range (Fig. 4b). $\Delta f\text{CO}_2 (T_{obs} - T_{ave})$ and $\Delta Nf\text{CO}_2 (T_{ave}, S_{ave})$ showed reversed distributions (Figs. 4a and c). Due to the anti-correlation between $\Delta f\text{CO}_2 (T_{obs} - T_{ave})$ and $\Delta Nf\text{CO}_2 (T_{ave}, S_{ave})$, surface $f\text{CO}_2$ was similar with that in au-

tumn in spite of the much lower SST. $\text{TER}_{\text{spatial}}$ in winter was 0.45 ± 0.18 (Fig. 4d), showing SST and SSS were not the primary factors to control the spatial distribution of surface $f\text{CO}_2$ like in summer. In winter, the surface mixed layer was deeper than 100 m in the study area (Fig. 6), implying active vertical mixing within the upper 100 m. Active mixing might have led to an increase in surface $f\text{CO}_2$, which could have offset the decrease due to lower SST. Higher surface $f\text{CO}_2$ was observed in the northwestern part of the study region, where the surface mixed layer was deeper than in other areas and surface chlorophyll a concentrations were lowest. Highest $\Delta Nf\text{CO}_2 (T_{ave}, S_{ave})$ in the northwestern part implied strong vertical mixing and/or weak biological activity. Lower surface $f\text{CO}_2$ was found at the southern and eastern parts of the study area, where surface chlorophyll a concentrations were relatively high. $\Delta Nf\text{CO}_2 (T_{ave}, S_{ave})$ in the southern and eastern parts were negative, representing relatively high biological activity. $\Delta Nf\text{CO}_2 (T_{ave}, S_{ave})$ was vaguely correlated with surface chlorophyll a (Fig. 5). In winter, surface $f\text{CO}_2$ was influenced, to some degree, by biological activity.

3.3 Factors Influencing the Seasonal Variability of Surface $f\text{CO}_2$

During the four seasonal surveys, the spatial mean SST showed a large variation of 13.2°C, while the spatial mean SSS showed a variation of 1.32 (Table 1). To validate the major influences of SST and SSS on surface $f\text{CO}_2$, we plotted the $\text{TER}_{\text{seasonal}}$ for the four seasonal surveys (Fig. 4e). $\text{TER}_{\text{seasonal}}$ were 0.50 ± 0.09 , 0.79 ± 0.08 , 0.68 ± 0.05 , and

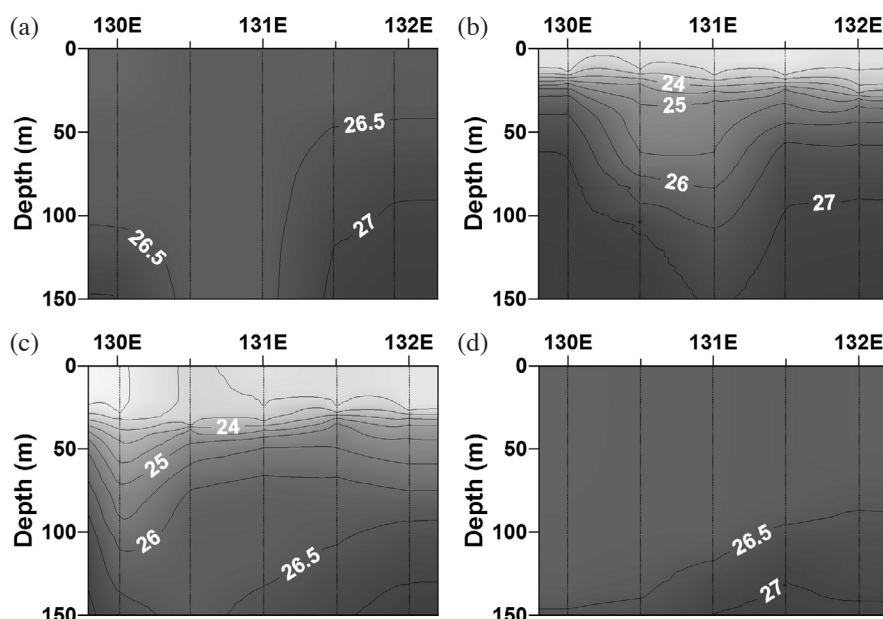


Fig. 6. Vertical distributions of density (σ_θ) from the surface to 150 m depth along Line D (37°N) from 130 to 132°E in April 2006 (a), August 2007 (b), October 2008 (c) and February 2008 (d).

Table 1. Seasonal surface water properties of the study area.

Seasons	SST (°C)	SSS	Surface $f\text{CO}_2$ (μatm)	Potential Energy Anomaly (J m^{-2})
Spring	10.73 ± 0.44	34.38 ± 0.08	309.4 ± 29.7	0.25 ± 0.28
Summer	23.87 ± 0.93	33.33 ± 0.27	371.5 ± 26.3	4.22 ± 0.31
Autumn	22.26 ± 0.67	33.06 ± 0.26	320.3 ± 10.5	3.85 ± 0.71
Winter	11.90 ± 1.12	34.15 ± 0.11	333.3 ± 13.4	0.18 ± 0.22

0.40 ± 0.02 in the spring, summer, autumn, and winter, respectively. SST and SSS played major roles to control surface $f\text{CO}_2$ in autumn and especially in summer. In the northern reaches of the South China Sea, however, the seasonal variations of surface $f\text{CO}_2$ were mainly influenced by the seasonal variations of SST (Zhai et al. 2005). In the northern East China Sea, where the Kuroshio Current passed through, the seasonal variations in surface $f\text{CO}_2$ were affected by the seasonal changes in SST (Shim et al. 2007).

The measured surface $f\text{CO}_2$ values in spring and winter were not significantly different from those in summer and autumn, despite the large differences in SST (Table 1). Considering only the temperature effect of $4.23\% \text{ } ^\circ\text{C}^{-1}$ (Takahashi et al. 1993), the surface $f\text{CO}_2$ would show a difference of about $200 \mu\text{atm}$ between winter and summer. However, the surface $f\text{CO}_2$ varied seasonally by $62 \mu\text{atm}$ (Table 1). The small seasonal variability of surface $f\text{CO}_2$ resulted from several processes, such as vertical and lateral mixing, biological activity, and sea-air CO_2 exchange (Ishii et al. 2001; Ríos et al. 2005; Shim et al. 2006). We plotted the relationships among $\Delta\text{N}f\text{CO}_2 (T_{ave}, S_{ave})$, SST, and SSS obtained during the four seasonal surveys (Fig. 7). A good inverse relationship between $\Delta\text{N}f\text{CO}_2 (T_{ave}, S_{ave})$ and SST in winter represented non-thermodynamic increment of surface $f\text{CO}_2$ by vertical mixing.

To elucidate the effects of vertical mixing on the surface $f\text{CO}_2$, the degree of stratification in the water column was calculated using the potential energy anomaly (PEA; Simpson et al. 1977; Shim et al. 2007). The low PEA indicated that the water column was unstable and well mixed. PEA was an order of magnitude higher in summer and autumn than in winter and spring (Table 1), indicating that the water column was unstable and well mixed in winter and spring. Low $\text{TER}_{\text{seasonal}}$ in winter and spring were consistent with low PEA. In winter and spring, therefore, the active vertical mixing brought CO_2 -rich subsurface waters to the surface, and thus caused the high surface $f\text{CO}_2$. Shim et al. (2007) explained the high surface $f\text{CO}_2$ observed in the East China Sea during spring and autumn by vertical mixing with CO_2 -rich water masses. Consequently, the small seasonal variability of surface $f\text{CO}_2$ was ascribed to the high surface $f\text{CO}_2$ due to active vertical mixing in winter and spring.

The Tsushima Warm Current entered the East Sea through the Korea/Tsushima Strait, transporting warm and

salty water into the study area (Chang et al. 2004). The Tsushima Warm Current branched from the Kuroshio Current and passed through the East China Sea before entering the study area. Kim et al. (2012) measured the surface $f\text{CO}_2$ in the northern East China Sea during four seasons; the spatial mean $f\text{CO}_2$ values were $311 \pm 31 \mu\text{atm}$ in spring, $309 \pm 53 \mu\text{atm}$ in summer, $376 \pm 37 \mu\text{atm}$ in autumn, and $335 \pm 17 \mu\text{atm}$ in winter. To identify the effects of lateral advection on the surface $f\text{CO}_2$, the spatial mean surface $f\text{CO}_2$ values measured in the study area were compared with those in the East China Sea during four seasons (Table 1). In winter and spring, the surface $f\text{CO}_2$ values measured in the study area were rather similar to those in the East China Sea. However, they were somewhat higher in summer and lower in autumn than those in the East China Sea. In summer, the Tsushima Warm Current Water with lower surface $f\text{CO}_2$ was transported into the study area. A relationship between $\Delta\text{N}f\text{CO}_2 (T_{ave}, S_{ave})$ and SSS in summer represented decline of non-thermodynamic changes on surface $f\text{CO}_2$ by intrusion of low-salinity and low- $f\text{CO}_2$ waters into the study area. Therefore, the small seasonal variability of surface $f\text{CO}_2$ resulted from the lateral transport of water masses with lower surface $f\text{CO}_2$ in summer.

In Fig. 5, the relationship was random, indicating that the seasonal variation of the surface $f\text{CO}_2$ was not affected by biological activities. The primary production estimated in the study area also showed little seasonal variation (Noh, personal communication). Therefore, the small seasonal variability of surface $f\text{CO}_2$ was not related to the biological activity.

Surface $f\text{CO}_2$ is also influenced by the sea-air CO_2 exchange. The changes in surface $f\text{CO}_2$ due to sea-air CO_2 exchange were quantitatively estimated from the mean seasonal mixed layer depths (70, 25, 50, and 92 m in spring, summer, autumn, and winter, respectively), surface mean DIC ($2100 \mu\text{mole kg}^{-1}$), and the Revelle factor (10). Values of 19.3, -1.6, 10.3, and $20.2 \mu\text{atm}$ were found for spring, summer, autumn, and winter, respectively. The increase in surface $f\text{CO}_2$ due to sea-air CO_2 exchange was largest in winter, the season with the highest CO_2 influx (Table 2). In summer, however, the surface $f\text{CO}_2$ decreased slightly by CO_2 outflux. Therefore, the small seasonal variability of surface $f\text{CO}_2$ was influenced, to some extent, by the sea-air CO_2 exchange.

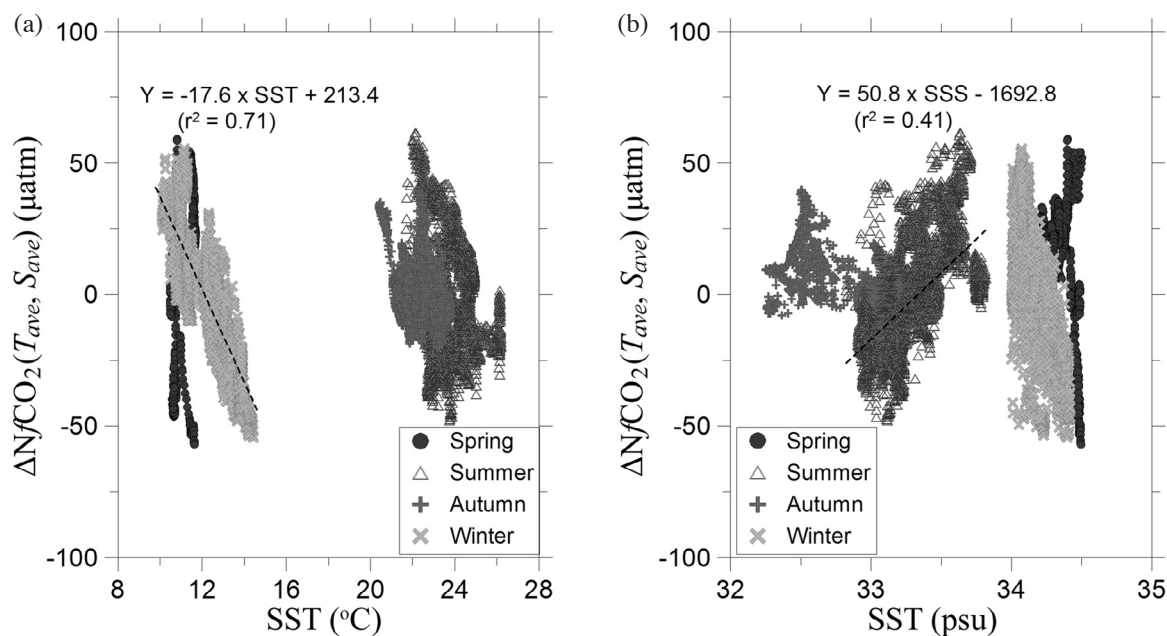


Fig. 7. Relationships between $\Delta f\text{CO}_2(T_{ave}, S_{ave})$ and SST (a) and SSS (b) during the four seasonal surveys.

Table 2. Sea-air differences of CO_2 fugacity ($\Delta f\text{CO}_2$), wind speeds, and sea-air CO_2 flux in the Ulleung Basin of the East Sea during the four seasonal observations.

Seasons	$\Delta f\text{CO}_2^a$ (μatm)	Wind Speed ^b (m sec^{-1})	Sea-air CO_2 Flux ^c ($\text{mmol C m}^{-2} \text{day}^{-1}$)
Spring	-62.3 ± 32.4	8.10 ± 1.70	-10.4 ± 5.43
Summer	2.51 ± 22.1	6.50 ± 2.88	0.26 ± 2.29
Autumn	-55.0 ± 9.96	5.31 ± 2.34	-3.83 ± 0.70
Winter	-48.9 ± 13.4	10.3 ± 5.04	-13.3 ± 3.62
Annual mean			-6.78 ± 3.46 ($-2.47 \pm 1.26 \text{ mol m}^{-2} \text{yr}^{-1}$)

^a Mean $\Delta f\text{CO}_2$ along the cruise tracks expressed as the mean \pm standard deviation (S.D.).

^b Mean wind speed of the study area ($35 \sim 37.5^\circ\text{N}$, $129 \sim 132^\circ\text{E}$) from QuikSCAT satellite data during each observation period, expressed as the mean \pm S.D.

^c Mean sea-air CO_2 fluxes based on the transfer coefficient of Wanninkhof (1992), expressed as the mean \pm S.D. Positive values represent CO_2 emission from the sea to the atmosphere, while negative values represent CO_2 absorption from the atmosphere to the sea.

3.4 Sea-Air CO_2 Flux

Table 2 shows the averaged sea-air differences of CO_2 fugacity ($\Delta f\text{CO}_2$), wind speeds, and calculated sea-air CO_2 fluxes for the four seasons. The CO_2 fluxes had large seasonal variation. The Ulleung Basin of the East Sea was a sink of atmospheric CO_2 in spring, autumn, and winter, but a small source of CO_2 to the atmosphere in summer.

In spring, the CO_2 influx (negative sign) was calculated to be $10.4 \pm 5.43 \text{ mmol m}^{-2} \text{day}^{-1}$. The lowest $\Delta f\text{CO}_2$ was observed in spring among the four seasons, probably due to the spring phytoplankton bloom. Thus, the large CO_2 influx in spring resulted from high biological activities. The calculated CO_2 influx was somewhat higher than that ($5.9 \text{ mmol m}^{-2} \text{day}^{-1}$) calculated in the southern part of the East Sea during April (Oh 1998).

In summer, the Ulleung Basin of the East Sea acted as a source of CO_2 to the atmosphere, with CO_2 flux of $0.26 \pm 2.29 \text{ mmol m}^{-2} \text{day}^{-1}$, which was almost the same as that ($0.33 \pm 2.48 \text{ mmol m}^{-2} \text{day}^{-1}$) estimated in July 2005 (Choi et al. 2011). The CO_2 outflux was also rather similar to that ($1.7 \text{ mmol m}^{-2} \text{day}^{-1}$) calculated for the southern part of the East Sea in August (Oh 1998).

In autumn, the CO_2 influx was calculated to be $3.83 \pm 0.70 \text{ mmol m}^{-2} \text{day}^{-1}$. The autumn $\Delta f\text{CO}_2$ was similar to that in spring, but the autumn CO_2 influx was less than half that in spring due to the low wind speed (Table 2). The CO_2 influx was quite similar to that ($2.9 \text{ mmol m}^{-2} \text{day}^{-1}$) calculated in the southern East Sea in October (Oh 1998).

The largest CO_2 influx ($13.3 \pm 3.62 \text{ mmol m}^{-2} \text{day}^{-1}$) was estimated in winter (Table 2). This high CO_2 influx was mainly attributable to high wind speeds in winter, because

the winter $\Delta f\text{CO}_2$ was higher than that in spring or autumn (Table 2). The winter CO_2 influx was somewhat lower than that ($17.4 \text{ mmol m}^{-2} \text{ day}^{-1}$) calculated for the southern part of the East Sea in February (Oh 1998).

The annual integrated sea-air CO_2 flux in the Ulleung Basin of the East Sea was $-2.47 \pm 1.26 \text{ mol m}^{-2} \text{ yr}^{-1}$ (Table 2), quite similar to the previous estimate ($-2.2 \text{ mol m}^{-2} \text{ yr}^{-1}$) for the southern East Sea (Oh 1998). The annual CO_2 uptake rate in this study area was considerably larger than the estimate for worldwide continental shelves ($-1.1 \text{ mol m}^{-2} \text{ yr}^{-1}$; Chen and Borges 2009) and the global mean ($-0.51 \text{ mol m}^{-2} \text{ yr}^{-1}$; Takahashi et al. 2009). Kim et al. (2012) reported that the annual sea-air CO_2 flux in the northern East China Sea was $-2.2 \pm 2.1 \text{ mol m}^{-2} \text{ yr}^{-1}$, which is comparable to our result. Therefore, the Ulleung Basin of the East Sea, like the East China Sea, acts as a strong sink of atmospheric CO_2 .

4. CONCLUSIONS

Observations from four seasonal cruises showed that the Ulleung Basin of the East Sea acts as a strong sink for atmospheric CO_2 . The sea-air CO_2 flux displayed large seasonal variation, with CO_2 emitted to the atmosphere in summer and absorbed from the atmosphere in other seasons. This finding is consistent with modeling results showing the East Sea emitting CO_2 into the atmosphere from June to September and absorbing CO_2 from October through May (Oh 1998; Kang 1999). In the Ulleung Basin of the East Sea, the seasonal variation of surface $f\text{CO}_2$ could not be explained solely by seasonal changes in SST and SSS. Considering only the temperature effect of $4.23\% \text{ }^\circ\text{C}^{-1}$, the surface $f\text{CO}_2$ would show a difference of about $200 \text{ } \mu\text{atm}$ between winter and summer, but the surface $f\text{CO}_2$ varied only by $62 \text{ } \mu\text{atm}$. The small seasonal variability of surface $f\text{CO}_2$ was attributed to the high surface $f\text{CO}_2$ due to the active vertical mixing in winter, the lateral transport of water masses with the lower surface $f\text{CO}_2$ in summer, and the sea-air CO_2 exchange. The Ulleung Basin of the East Sea adsorbed atmospheric CO_2 at an annual rate of $2.47 \pm 1.26 \text{ mol m}^{-2} \text{ yr}^{-1}$, which was comparable with the previous model result ($-2.2 \text{ mol m}^{-2} \text{ yr}^{-1}$) for the southern East Sea (Oh 1998). The annually integrated CO_2 flux for worldwide continental shelves was $-1.1 \text{ mol m}^{-2} \text{ yr}^{-1}$ (Chen and Borges 2009), which was less than half the CO_2 influx estimated for the Ulleung Basin of the East Sea. Therefore, the Ulleung Basin of the East Sea acts as a strong sink for atmospheric CO_2 compared to other continental shelves.

Acknowledgements We are indebted to the captain and crew of the R/V *Eardo* for their outstanding help with all our shipboard operations. We also thank Drs. Chang-Woong Shin, Jae-Hoon Noh, Eun-Jin Yang, and Hyung-Gu Kang for assistance with the fieldwork. This work was supported by the MLTM R&D projects (PM56600 and PMS227D).

REFERENCES

- Borges, A. V., B. Delille, and M. Frankignoulle, 2005: Budgeting sinks and sources of CO_2 in the coastal ocean: Diversity of ecosystems counts. *Geophys. Res. Lett.*, **32**, L14601, doi: 10.1029/2005GL023053. [\[Link\]](#)
- Chang, K. I., N. G. Hogg, M. S. Suk, S. K. Byun, Y. G. Kim, and K. Kim, 2002: Mean flow and variability in the southwestern East Sea. *Deep-Sea Res. I*, **49**, 2261-2279, doi: 10.1016/S0967-0637(02)00120-6. [\[Link\]](#)
- Chang, K. I., W. J. Teague, S. J. Lyu, H. T. Perkins, D. K. Lee, D. R. Watts, Y. B. Kim, D. A. Mitchell, C. M. Lee, and K. Kim, 2004: Circulation and currents in the southwestern East/Japan Sea: Overview and review. *Prog. Oceanogr.*, **61**, 105-156, doi: 10.1016/j.pocan.2004.06.005. [\[Link\]](#)
- Chen, C., J. Zhu, R. C. Beardsley, and P. J. S. Franks, 2003: Physical-biological sources for dense algal blooms near the Changjiang River. *Geophys. Res. Lett.*, **30**, 1515, doi: 10.1029/2002GL016391. [\[Link\]](#)
- Chen, C. T. A. and A. V. Borges, 2009: Reconciling opposing views on carbon cycling in the coastal ocean: Continental shelves as sinks and near-shore ecosystems as sources of atmospheric CO_2 . *Deep-Sea Res. II*, **56**, 578-590, doi: 10.1016/j.dsr2.2009.01.001. [\[Link\]](#)
- Choi, S. H., D. Kim, J. H. Shim, and H. S. Min, 2011: The spatial distribution of surface $f\text{CO}_2$ in the southwestern East Sea/Japan Sea during summer 2005. *Ocean Sci. J.*, **46**, 13-21, doi: 10.1007/s12601-011-0002-2. [\[Link\]](#)
- Ishii, M., H. Y. Inoue, H. Matsueda, S. Saito, K. Fushimi, K. Nemoto, T. Yano, H. Nagai, and T. Midorikawa, 2001: Seasonal variation in total inorganic carbon and its controlling processes in surface waters of the western North Pacific subtropical gyre. *Mar. Chem.*, **75**, 17-32, doi: 10.1016/S0304-4203(01)00023-8. [\[Link\]](#)
- Kang, D. J., 1999: A study on the carbon cycle in the East Sea. Ph.D Thesis, Seoul National University, 159 pp, Seoul, Korea.
- Kim, D., S. H. Choi, J. H. Shim, K. H. Kim, and C. H. Kim, 2012: Seasonal variability of sea-air CO_2 fluxes in the northern East China Sea. *J. Mar. Syst.*, submitted.
- Liu, K. K., K. Iseki, and S.-Y. Chao, 2000: Continental margin carbon fluxes. In: Hanson, R. B., H. W. Ducklow, and J. G. Field (Eds.), *The Changing Ocean Carbon Cycle: A Midterm Synthesis of the Joint Global Ocean Flux Study*, Cambridge University Press, Cambridge, 187-239.
- Oh, D. C., 1998: A Study on the Characteristics of $f\text{CO}_2$ Distributions and CO_2 Flux at the Air-sea Interface in the Seas around Korea. Master Thesis, Seoul National University, 92 pp, Seoul, Korea.
- Omar, A. M., T. Johannessen, A. Olsen, S. Kaltin, and F. Rey, 2007: Seasonal and interannual variability of the

- air-sea CO_2 flux in the Atlantic sector of the Barents Sea. *Mar. Chem.*, **104**, 203-213, doi: 10.1016/j.marchem.2006.11.002. [[Link](#)]
- Park, G. H., K. Lee, P. Tishchenko, D. H. Min, M. J. Warner, L. D. Talley, D. J. Kang, and K. R. Kim, 2006: Large accumulation of anthropogenic CO_2 in the East (Japan) Sea and its significant impact on carbonate chemistry. *Global Biogeochem. Cycles*, **20**, GB4013, doi: 10.1029/2005GB002676. [[Link](#)]
- Ríos, A. F., F. F. Pérez, M. Álvarez, L. Mintrop, M. González-Dávila, J. M. Santana Casiano, N. Lefèvre, and A. J. Watson, 2005: Seasonal sea-surface carbon dioxide in the Azores area. *Mar. Chem.*, **96**, 35-51, doi: 10.1016/j.marchem.2004.11.001. [[Link](#)]
- Shim, J. H., Y. C. Kang, D. Kim, and S. H. Choi, 2006: Distribution of net community production and surface $p\text{CO}_2$ in the Scotia Sea, Antarctica, during austral spring 2001. *Mar. Chem.*, **101**, 68-84, doi: 10.1016/j.marchem.2005.12.007. [[Link](#)]
- Shim, J. H., D. Kim, Y. C. Kang, J. H. Lee, S. T. Jang, and C. H. Kim, 2007: Seasonal variations in $p\text{CO}_2$ and its controlling factors in surface seawater of the northern East China Sea. *Cont. Shelf Res.*, **27**, 2623-2636, doi: 10.1016/j.csr.2007.07.005. [[Link](#)]
- Simpson, J. H., D. G. Hughes, and N. C. G. Morris, 1977: The relation of seasonal stratification to tidal mixing on the continental shelf. In: Angel, M. (Ed.), *Voyage of Discovery*, 327-340.
- Takahashi, T., J. Olafsson, J. G. Goddard, D. W. Chipman, and S. C. Sutherland, 1993: Seasonal variation of CO_2 and nutrients in the high-latitude surface oceans: A comparative study. *Global Biogeochem. Cycles*, **7**, 843-878, doi: 10.1029/93GB02263. [[Link](#)]
- Takahashi, T., S. C. Sutherland, R. Wanninkhof, C. Sweeney, R. A. Feely, D. W. Chipman, B. Hales, G. Friederich, F. Chavez, C. Sabine, A. Watson, D. C. E. Bakker, U. Schuster, N. Metzl, H. Yoshikawa-Inoue, M. Ishii, T. Midorikawa, Y. Nojiri, A. Körtzinger, T. Steinhoff, M. Hoppema, J. Olafsson, T. S. Arnarson, B. Tilbrook, T. Johannessen, A. Olsen, R. Bellerby, C. S. Wong, B. Delille, N. R. Bates, and H. J. W. de Baar, 2009: Climatological mean and decadal change in surface ocean $p\text{CO}_2$, and net sea-air CO_2 flux over the global oceans. *Deep-Sea Res. II*, **56**, 554-577, doi: 10.1016/j.dsr2.2008.12.009. [[Link](#)]
- Thomas, H., Y. Bozec, K. Elkalay, and H. J. W. de Baar, 2004: Enhanced open ocean storage of CO_2 from shelf sea pumping. *Science*, **304**, 1005-1008, doi: 10.1126/science.1095491. [[Link](#)]
- Uda, M., 1934: Oceanographic conditions in the Japan Sea and its adjacent waters (the result of simultaneous oceanographical investigations in the Japan Sea and its adjacent water in May and June, 1932). *J. Imperial Fish. Expedition Station*, **5**, 57-190. (in Japanese)
- Wang, S. L. and C. T. A. Chen, 1996: Comparison of seawater carbonate parameters in the East China Sea and the Sea of Japan. *La mer*, **34**, 131-136.
- Wanninkhof, R., 1992: Relationship between wind speed and gas exchange over the ocean. *J. Geophys. Res.*, **97**, 7373-7382, doi: 10.1029/92JC00188. [[Link](#)]
- Weiss, R. F., 1974: Carbon dioxide in water and seawater: The solubility of a non-ideal gas. *Mar. Chem.*, **2**, 203-215, doi: 10.1016/0304-4203(74)90015-2. [[Link](#)]
- Yamada, K., J. Ishizaka, and H. Nagata, 2005: Spatial and temporal variability of satellite primary production in the Japan Sea from 1998 to 2002. *J. Oceanogr.*, **61**, 857-869, doi: 10.1007/s10872-006-0005-2. [[Link](#)]
- Yoo, S. and J. Park, 2009: Why is the southwest the most productive region of the East Sea/Sea of Japan? *J. Mar. Syst.*, **78**, 301-315, doi: 10.1016/j.jmarsys.2009.02.014. [[Link](#)]
- Zhai, W., M. Dai, W. J. Cai, Y. Wang, and H. Hong, 2005: The partial pressure of carbon dioxide and air-sea fluxes in the northern South China Sea in spring, summer and autumn. *Mar. Chem.*, **96**, 87-97, doi: 10.1016/j.marchem.2004.12.002. [[Link](#)]